

Positively charged supported lipid bilayer formation on gold surfaces for neuronal cell culture

Sung-Eun Choi, Kyrylo Greben, Roger Wördenweber, and Andreas Offenhäusser

Citation: *Biointerphases* **11**, 021003 (2016); doi: 10.1116/1.4945306

View online: <http://dx.doi.org/10.1116/1.4945306>

View Table of Contents: <http://scitation.aip.org/content/avs/journal/bip/11/2?ver=pdfcov>

Published by the AVS: Science & Technology of Materials, Interfaces, and Processing

Articles you may be interested in

[Dynamic and mechanical properties of supported lipid bilayers](#)

J. Chem. Phys. **144**, 154904 (2016); 10.1063/1.4947038

[Optimization of Brownian ratchets for the manipulation of charged components within supported lipid bilayers](#)

Appl. Phys. Lett. **106**, 183703 (2015); 10.1063/1.4919801

[Real-time detection of lipid bilayer assembly and detergent-initiated solubilization using optical cavities](#)

Appl. Phys. Lett. **106**, 071103 (2015); 10.1063/1.4908270

[A biomimetic mechanism for antibody immobilization on lipid nanofibers for cell capture](#)

Appl. Phys. Lett. **101**, 193701 (2012); 10.1063/1.4766191

[Self-formation of bilayer lipid membranes on agarose-coated silicon surfaces studied by simultaneous electrophysiological and surface infrared spectroscopic measurements](#)

Appl. Phys. Lett. **94**, 243906 (2009); 10.1063/1.3140206

Positively charged supported lipid bilayer formation on gold surfaces for neuronal cell culture

Sung-Eun Choi, Kyrylo Greben, Roger Wördenweber, and Andreas Offenhäusser^{a)}

Peter Grünberg Institute (PGI-8) and Institute of Complex Systems (ICS-8), Forschungszentrum Jülich GmbH, Jülich 52428, Germany

(Received 12 February 2016; accepted 22 March 2016; published 6 April 2016)

Supported lipid bilayers are widely used as cell membrane models and sensor platforms, but the usage on gold surface needs additional surface modification or optimized experimental conditions. In this work, the authors show lipid bilayer formation on plasma activated gold surfaces in physiological conditions without any other modification if at least 30% positively charged lipids are present. Details of bilayer formation from small unilamellar vesicles were monitored using quartz crystal microbalance with dissipation in both basic and acidic environment. The authors also confirmed that this positively charged bilayer system can sustain primary cortical neuron growth and lipid transfer. This method will provide simple means to construct biomimetic interface on gold electrodes. © 2016 American Vacuum Society. [<http://dx.doi.org/10.1116/1.4945306>]

I. INTRODUCTION

Cell membranes are composed of lipid bilayer, proteins, cholesterol, and carbohydrates and indispensable for cell-cell interaction, transport of ions and molecules, and signal transduction.¹ To study cell membranes, lipid bilayers deposited on solid surface² [supported lipid bilayers (SLB)] are widely used as a simplified model cell membrane due to the two dimensional lateral fluidity and simplified compositions by using purified components.³ SLB are physically stable and can be easily characterized by surface sensitive detection techniques^{4,5} for biosensors⁶ and cell biology studies.⁷ The biomimetic feature of SLB can also provide natural cell culture environment to study the protein and cytoskeleton organization^{8–10} and lipid domain formation.¹¹ Intracellular potential measurement was demonstrated using SLB as an interface between transistors and cells.¹²

SLB on gold surface are widely used because the gold surface allows well-known chemical modification and is suitable for electrical and optical measurements.^{13–15} Many techniques like electrochemistry,^{16–20} and surface plasmon resonance,^{21,22} not to mention microelectrode arrays, have employed gold surfaces for cellular interaction studies. However, it is well known that the formation of SLB on the gold surface from lipid vesicles is restricted.^{23–26} To prepare SLB, self-assembled monolayer of thiol is the most popular surface modification method to change the surface hydrophilicity, but this hinders electrical access to other molecules.^{27–30} Several other approaches based on vesicle fusion^{31–33} were developed to induce vesicle rupture and SLB formation on bare gold surfaces by using thiol labeled lipids in lipid vesicles,^{34,35} optimizing buffer,^{30,36} inserting peptide to rupture adsorbed vesicles,³⁷ and organic solvent assisted method.³⁸

As SLB formation depends on many experimental variables like pH, hydrophilicity, ionic concentration, osmotic pressure, vesicle size, and temperature,^{24,39} optimal conditions

should be used for different surfaces and lipid compositions. To use SLB for various biological studies, various biological components such as proteins and lipids have been incorporated in lipid vesicles and bilayer. For this reason, fabrication methods which work under physiological conditions without surface treatment are needed.

Here, we show that positively charged small unilamellar lipid vesicles rupture and form bilayers on gold surfaces without any additional surface modification in physiological condition. To observe the kinetic behavior of vesicle rupture and SLB formation on gold surface, quartz crystal microbalance with dissipation (QCM-D) monitoring system was used. In addition to bilayer formation, we demonstrate that positively charged SLB on gold surfaces also supports primary neuronal cell growth.

II. EXPERIMENT

A. Materials

1-palmitoyl-2-oleoyl-sn-glycero-3-phosphocholine (POPC, zwitterionic) and 1,2-dioleoyl-3-trimethylammonium-propane (DOTAP, positive) were purchased from Avanti Polar Lipids, Inc. Oregon green[®] 488 DHPE, Neurabasal medium, B27 supplement, L-glutamine, and Calcein AM were obtained from Invitrogen. Poly-D-lysine (PDL) and salts for phosphate buffer saline (PBS), HCl, and NaOH solution were purchased from Sigma-Aldrich GmbH. Hellmanex[®] III for the cleaning of the glass coverslips was bought from Hellma Analytics. For the zeta potential measurements and cell culture, gold (Au) layers with a thickness of 100 nm were deposited via sputter technology on silicon wafers using a 10 nm titanium layer as an adhesion layer.

B. Lipid vesicle preparation

Lipids were dissolved in chloroform with the desired ratio and dried on the glass vial using a stream of N₂. 0.2% Oregon green 488 DHPE was added when fluorescence observation was needed. The thin lipid film was kept in a

^{a)}Electronic mail: a.offenhaeuser@fz-juelich.de

vacuum chamber for 1 h to remove any trace of the solvent. Subsequently the lipids were rehydrated to 5 mg/ml with PBS and extruded using Avanti mini extruder (Avanti polar Lipid, Inc.) through 30 nm diameter pores of a polycarbonate membrane. The lipid stock solution was kept in a fridge for less than 1 week.

The zeta potential of the lipid vesicles was measured using a Zetasizer Nano ZS instrument (Malvern Instruments, Malvern, UK) with a folded capillary cell. All measurements were done at 25 °C with 0.1 mg/ml lipid vesicle solution in PBS. The electrophoretic mobility of vesicles were converted to zeta potential using the Smoluchowski equation.⁴⁰

C. QCM-D measurement

A Q-sense E4 instrument, equipped with open modules and QSOFT software (BiolinScientific/Q-Sense, Sweden), was used for the monitoring of the lipid bilayer formation. Au coated AT-cut quartz crystals with a fundamental frequency of 5 MHz (BiolinScientific/Q-Sense, Sweden) were cleaned with oxygen plasma (Diener Electronics) and immersed in a 5:1:1 solution of water, 25% ammonia, and 30% hydrogen peroxide for 20 min at 65 °C. These sensors were always again activated with the oxygen plasma before experiments. The as prepared lipid vesicle solution was diluted to 0.3 mg/ml in PBS, and, after stabilization, 1 ml of the solution was applied to the open chamber. After bilayer formation or vesicle adsorption, excess lipid vesicles were washed out with PBS. The measurements were done for $n = 1$ –13 overtones for at least three times. For clarity, all results displayed here are the representative result of 11th overtone. See supplementary material for average and standard deviation of final frequencies and dissipations.⁴¹ The pH of the buffer was adjusted by adding HCl or NaOH solution.

D. Streaming potential/streaming current measurements

For the analysis of the surface potential of gold surfaces, a modified electrokinetic analyzer SurPASS (Anton Paar Germany GmbH) was used. A pair of identical planar samples (10 × 10 mm) was placed in a clamping cell with gold surfaces facing each other, forming a microfluidic channel. The gap height of 100 μm between the two parallel-plane surfaces was kept to ensure laminar flow of the electrolyte. The detailed measurement principle is, for instance, described in Werner *et al.*⁴² Potassium chloride (KCl, 10 mM) was used as the working electrolyte solution. The pH value of the working electrolyte was changed in the range of 6–10 with potassium hydroxide (KOH, 50 mM) as the titration solution. To ensure the reproducibility and reliability of the measurement, an optimized measurement procedure was used.⁴³ Prior to each measurement, the samples were cleaned and activated in an oxygen plasma with the parameters 120 W, 0.8 mbar pressure, and 5 min duration.

E. Surface preparation for the cell culture

The gold surface was cleaned via the same procedure that was used for the QCM-D sensors. For cell culture control experiments on glass, coverslips (18 mm) were cleaned with a 2% Hellmanex solution and water in an ultrasonic bath. After cleaning, the coverslips were dried at 60 °C overnight and stored until use. All the substrates were treated with O₂ plasma and sterilized by UV for 30 min just before the experiments. The PDL was dissolved in PBS at 50 $\mu\text{g/ml}$, and the lipid solution was diluted to 0.3 mg/ml in PBS. These solutions were applied on the glass or on the gold surface. After 1 h, these substrates were rinsed with PBS and the cell culture media.

F. Cell culture

Rat embryonic cortical neurons were prepared as described before.⁴⁴ Briefly, primary cortical neurons were retrieved from pregnant Wistar rats at 18 days of gestation and suspended in 1 ml of neurobasal medium containing 1% B-27, 0.5 mM L-glutamine, and 50 $\mu\text{g/ml}$ gentamicin. These cells were plated on the substrate at a density of ~ 200 cells/ mm^2 . Half of the medium was changed 4 h after preparation and subsequently every 3–4 days. The experiments are approved by LANUV (Landesumweltamt für Natur, Umwelt und Verbraucherschutz Nordrhein-Westfalen, Recklinghausen, Germany, in accordance with §6 TierschG., §4 TSchG i.V. and §2 TierSchVerV).

G. Live cell staining

Calcein AM was diluted to 1:2000 in PBS, and the cell culture medium was changed to this solution. The cells were incubated for 1 h at 37 °C and washed with PBS. The number of live cells was obtained by counting Calcein AM stained cells in fluorescence images using IMAGEJ (National Institute of Health, USA).

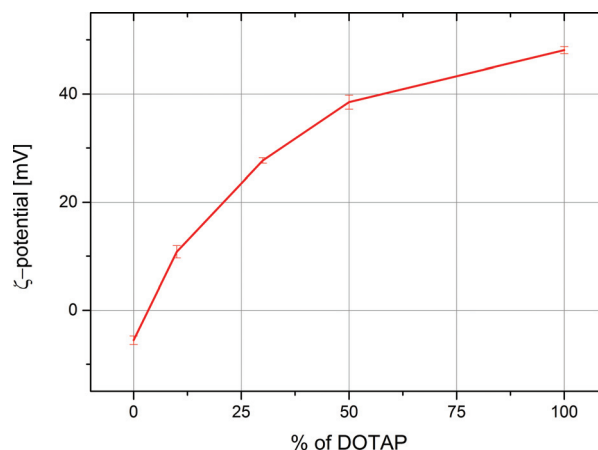


FIG. 1. Zeta potential of lipid vesicles with different ratio of POPC and DOTAP measured in PBS (pH 7.4).

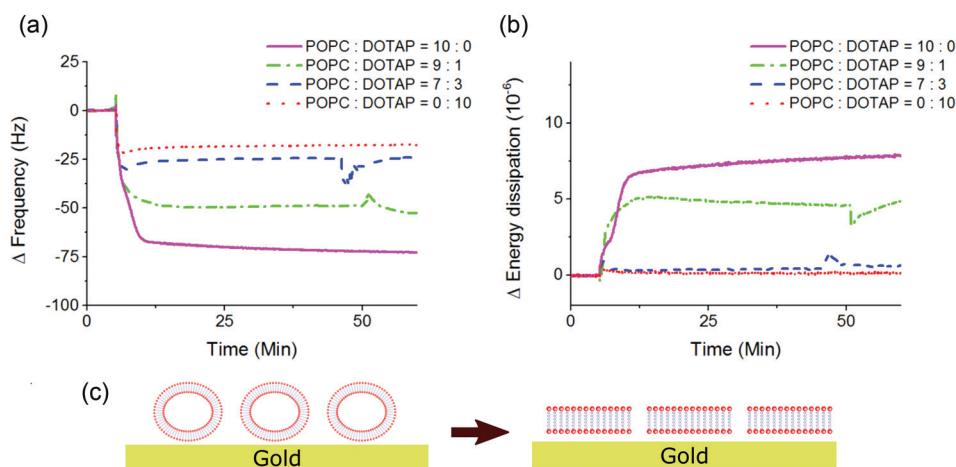


FIG. 2. QCM-D monitoring of positive charged and neutral vesicle adsorption on gold surface. Frequency (a) and energy dissipation (b) change are presented with different ratio of POPC and DOTAP in PBS. 1 ml of vesicle solution was added to the chamber for 5 min after stabilization, and excess vesicles were washed with PBS around 50 min. No change was observed after washing. (c) Schematic representation of lipid vesicle adsorption and rupture. The abrupt change comes from the pressure and temperature change when lipid solution and PBS buffer were applied in the open chamber directly using a pipette.

III. RESULTS AND DISCUSSION

A. Effect of different ratio of positive charged lipid vesicles

We first observed the bilayer formation on gold with different surface charge of liposomes by using a mixture of DOTAP [positive charged lipid in pH 7 (Ref. 45)] and POPC (zwitterionic lipid in pH 7). The zeta potential of liposomes increases with the ratio of DOTAP (Fig. 1).

In order to observe the adsorption and bilayer formation in real time, we used QCM-D, which is a powerful method to study the bilayer formation on solid surface in real time.²³ QCM-D provides mass (frequency change, Δf) and viscoelastic property (energy dissipation change, ΔD) on the sensor surface,⁴⁶ and it is particularly sensitive to the adsorption of water filled vesicles.⁴⁷

Figure 2 shows QCM-D signals for POPC and DOTAP lipid vesicle depositions on gold surfaces with various POPC and DOTAP ratios. The lipid vesicle solution was added after 5 min and excess vesicles were washed away with PBS after 40 min. Right after vesicle injection, vesicles attached on the surface as indicated by the decrease in frequency and increase in dissipation. After reaching an equilibrium state, typically $\Delta f \approx -25$ Hz and $\Delta D < 1 \times 10^{-6}$ can be observed for sensors fully covered by lipid bilayers.^{23,25,47} This can be seen for the highly charged lipid vesicles (over 30% DOTAP, red and blue curves in Fig. 2). The frequency minimum and energy dissipation maximum is not observed during bilayer formation, which is similar to reports for the deposition on SiO_2 surface.⁴⁸ This indicates that after the positively charged vesicles adsorb on gold surface, they rupture spontaneously without the support of any other additional forces like vesicle-vesicle interaction. On the contrary, neutral vesicles (0% DOTAP, solid magenta curve in Fig. 2) seem to form a lipid vesicle layer without the rupturing process, which is represented by significantly large change of frequency and dissipation. Total mass of adsorbed

lipid vesicle layer is larger than lipid bilayer because the buffer in the vesicles and bound to the vesicles also contributes to the mass change. And the elastic property of vesicles and surrounding molecules cause high energy dissipation generated by the shear stress from the oscillation of QCM-D. Thin layer such as lipid bilayer couples tightly to the surface, so energy dissipation is quite low.²³ The intermediate frequency and dissipation change observed for 10% DOTAP (dotted green curve in Fig. 2) can be interpreted as a formation of a mixture of lipid vesicles and bilayer on the gold surface.

Typically, vesicles start to rupture and form bilayers when the vesicle-surface interaction is strong enough to overcome the surface tension.^{49,50} The positive charge of lipid vesicles can lead to an attractive electrostatic interaction with the negatively charged gold surface. The negative charge of the gold surface was measured with streaming potential method (Fig. 3) and agrees with the literature.⁵¹ In addition, the number of charged lipid molecules in vesicles has a strong influence on the vesicle rupture process on the surface.⁵² As a consequence, the larger the charge of the lipids that are included in the vesicle, the stronger the interaction between the Au surface and the lipid vesicles.

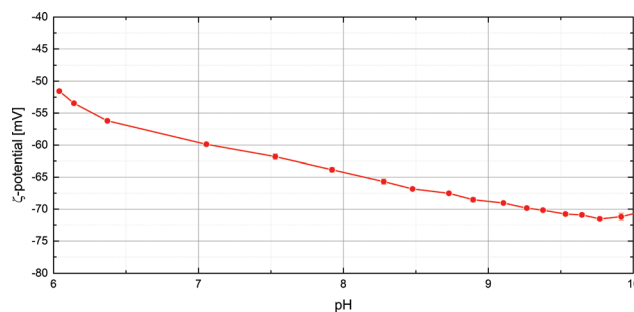


FIG. 3. Zeta-potential of gold surfaces in pH 6–10 KCl solution determined by streaming potential measurement.

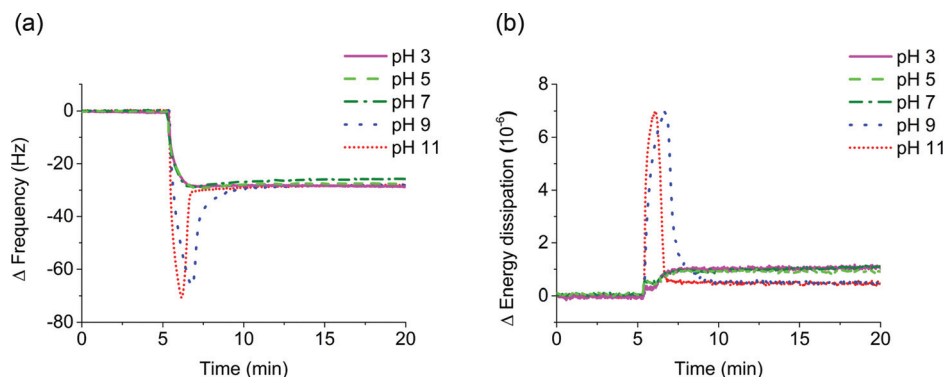


FIG. 4. Frequency (a) and energy dissipation (b) change of SLB formation for different pH values of the buffer solution. Lipid vesicles composed of POPC:DOTAP = 7:3 were applied on gold sensor surface at 5 min. In basic buffer (pH 9 and 11), a critical surface coverage had to be reached for SLB formation.

B. Influence of the pH on the bilayer formation

Next, we tested different pH values of PBS for the bilayer formation in order to change the electrostatic interaction. In acidic and neutral condition, positively charged vesicles rupture spontaneously as shown before in Fig. 2 and also in Fig. 4. However, in basic buffer (pH 9 and 11) vesicles do not rupture instantaneously although the Au surface is more negatively charged. This is counterintuitive because the negative surface charge should cause stronger electrostatic interaction. Increasing electrostatic interaction by lowering NaCl concentration did not show this difference (Fig. 5), but vesicles first have to reach a critical surface coverage before forming bilayers in basic condition. This two-step process (mass increase by vesicle adsorption until the critical concentration of vesicles is reached, followed by a decrease in the mass due to the rupture of the vesicles) in basic buffer (red and blue dotted curve in Fig. 4) indicates that, although the electrostatic vesicle–surface interaction is expected to be stronger than for the acidic or neutral buffer, a sufficiently large vesicle–vesicle interaction is required for the SLB formation.⁴⁸ An explanation might be that the electrostatic interaction in basic conditions might be reduced due to the screening of the positive charge of DOTAP by HPO_4^{2-} since this divalent counter ion (the dominant anionic ion in PBS) might effectively bind to DOTAP.^{53,54} Moreover, these

counter ion might also generate an entropic repulsion when vesicles approach the gold surface as reported by Zhu *et al.*⁵⁵ These effects might weaken the electrostatic adhesion force of the lipid to the surface.

C. Neuronal cell culture on SLB coated gold

As reported previously on glass surfaces, positively charged SLB are suitable for the adhesion and proliferation of neuronal cells.⁵⁶ Since positively charged lipids also form bilayers on gold surfaces, the same experimental procedures were used to construct SLB on gold for neuronal cell culture experiments. Primary neuronal cells were seeded on this gold supported SLB and cultured for 10 days and stained with Calcein AM (Fig. 6). Morphology and number of live cells on SLB were same as conventional PDL coating. While nitrogen head group of DOTAP shows cytotoxic effect when encapsulated for mammalian cell transfection,⁵⁷ cytotoxicity of DOTAP was not observed on this neuronal culture system. In contrast, without any coating or with only POPC vesicle layer on gold surfaces, cells did not attach and survive (see supplementary material for cells on POPC on gold surface).

Mixture of DOTAP and fusogenic lipid has been used to deliver deoxyribonucleic acid to cells⁵⁸ and for cell membrane functionalization.⁵⁹ To monitor if there is any lipid transfer from SLB to cells, fluorescent lipid (Oregon green

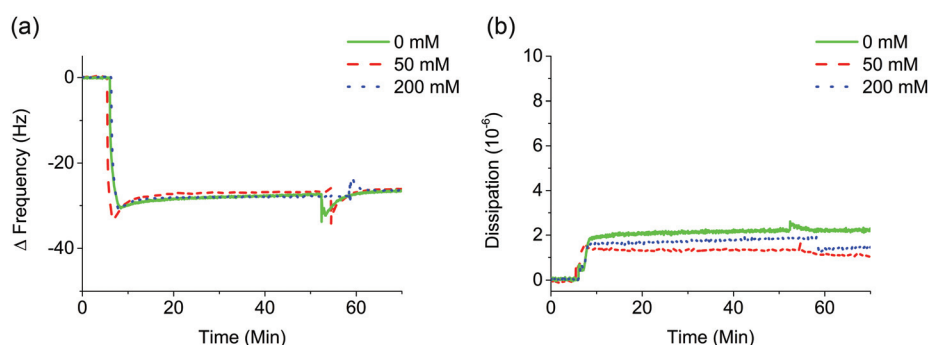


FIG. 5. Frequency (a) and energy dissipation (b) change of SLB formation for different concentration of NaCl in phosphate buffer solution (pH 7). Lipid vesicles composed of POPC:DOTAP = 7:3 were applied on gold sensor surface at 5 min.

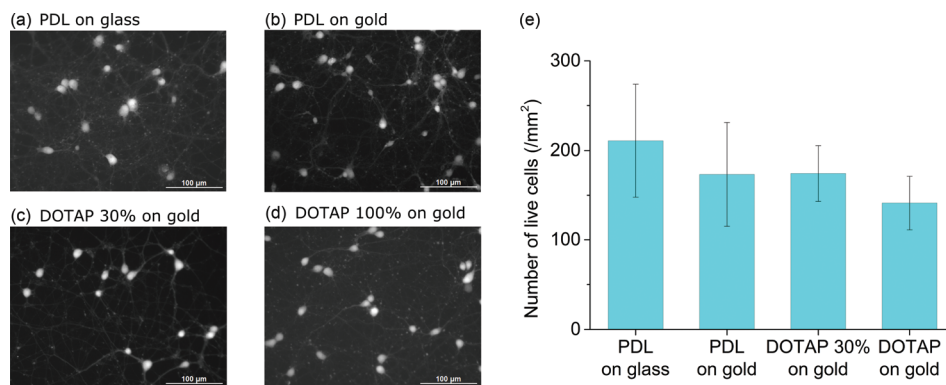


FIG. 6. (a)–(d)] Fluorescent microscopy images of primary cortical neurons on different surface treatments (DIV 10). Only live cells were stained with Calcein AM. (e) Numbers of live neuronal cells on SLBs on gold. Error bars represent standard deviation.

DHPE) was inserted in the SLB contains 30% and 100% DOTAP. Dead cells on those SLBs showed bright fluorescence which indicates that spontaneous lipid transfer⁶⁰ has occurred (Fig. 7). Live cells on 30% DOTAP SLB did not show any fluorescence while plasma membrane of neurons on 100% DOTAP were fluorescent, which shows that neurons can resist spontaneous transfer at low DOTAP concentration. From these observations, we can infer that there is passive lipid transfer from SLB to cell membrane due to electrostatic interaction, but cells on 30% DOTAP SLB can inhibit the transfer or destroy the transferred lipids. But, on high DOTAP concentration, passive transfer originated from electrostatic interaction is faster than the cell's protective activity or DOTAP initiate other cellular endocytosis pathway. Further research is needed to illuminate the mechanism of lipid transfer and protective action of cells. So, lower concentration of DOTAP is better to provide inert surface for cell culture. Detailed study about the effect of transferred lipids on cells is needed to use the higher charged SLB as a cell membrane modification method.

IV. SUMMARY AND CONCLUSIONS

We demonstrated that positively charged lipid vesicles form lipid bilayers on bare gold surface in physiological condition and support neuronal cell growth. With sufficient positive charge, lipid vesicles rupture spontaneously on gold surfaces without any modification. The positively charged lipid possesses a strong enough electrostatic interaction with the gold surface for lipid vesicles to overcome the energy barrier in acidic and neutral solution. However, in basic buffer, the surface-vesicle interaction alone is not strong enough. Therefore, additional vesicle-vesicle interaction is necessary for the bilayer formation. Finally, the adhesion and growth of primary neuronal cells cultured on these positively charged SLBs on gold is comparable with that of conventional protein coatings. Our presented procedure could be used for the formation of biomimetic surfaces on micro/nanofabricated gold electrodes that can be used to measure electrical and optical signals of cellular interaction in biologically⁶¹ and physically^{62–64} diverse systems.

ACKNOWLEDGMENTS

The authors would like to thank to Vanessa Maybeck, Bettina Breuer, and Rita Fricke for their support with neuronal cell preparation and Agnes Csiszar for the use of Zetasizer. The work was supported by DFG Research Training Group (GRK) 1572 Bionik.

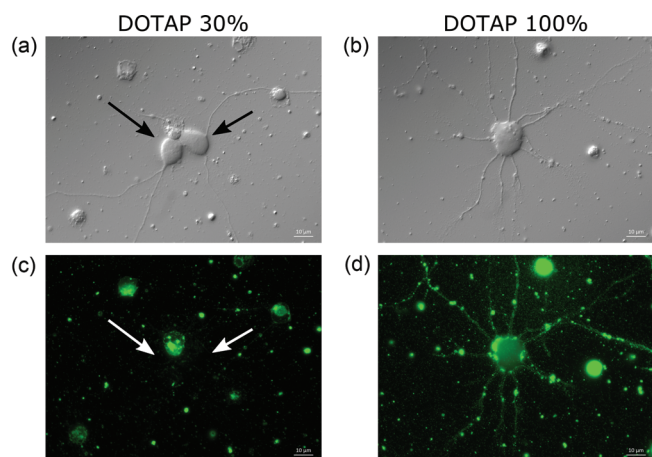


FIG. 7. DIC image [(a) and (b)] and fluorescence image [(c) and (d)] of neurons on SLB on gold (DIV 6). SLB contains Oregon green 488 DHPE (green fluorescence). [(a) and (c)] On DOTAP 30% SLB, only dead cells show fluorescence. Arrows indicate position of live cells. [(b) and (d)] On DOTAP 100% SLB, both live and dead cells show fluorescence.

- ¹A. A. Spector and M. A. Yorek, *J. Lipid Res.* **26**, 1015 (1985).
- ²L. K. Tamm and H. M. McConnell, *Biophys. J.* **47**, 105 (1985).
- ³M. Loose and P. Schwill, *J. Struct. Biol.* **168**, 143 (2009).
- ⁴E. Sackmann, *Science* **271**, 43 (1996).
- ⁵E. T. Castellana and P. S. Cremer, *Surf. Sci. Rep.* **61**, 429 (2006).
- ⁶M. Bally, K. Bailey, K. Sugihara, D. Grieshaber, J. Vörös, and B. Städler, *Small* **6**, 2481 (2010).
- ⁷C.-H. Yu and J. Groves, *Med. Biol. Eng. Comput.* **48**, 955 (2010).
- ⁸K. Salaita, P. M. Nair, R. S. Petit, R. M. Neve, D. Das, J. W. Gray, and J. T. Groves, *Science* **327**, 1380 (2010).
- ⁹X. Zhu, Z. Wang, A. Zhao, N. Huang, H. Chen, S. Zhou, and X. Xie, *Colloids Surf., B* **116**, 459 (2014).
- ¹⁰M. Andreasson-Ochsner, G. Romano, M. Hakanson, M. L. Smith, D. E. Leckband, M. Textor, and E. Reimhult, *Lab Chip* **11**, 2876 (2011).
- ¹¹C. Madwar, G. Gopalakrishnan, and R. B. Lennox, *Langmuir* **31**, 4704 (2015).

- ¹²B. Tian, T. Cohen-Karni, Q. Qing, X. Duan, P. Xie, and C. M. Lieber, *Science* **329**, 830 (2010).
- ¹³M. Stelzle, G. Weissmueller, and E. Sackmann, *J. Phys. Chem.* **97**, 2974 (1993).
- ¹⁴J. Homola, S. S. Yee, and G. Gauglitz, *Sens. Actuators, B* **54**, 3 (1999).
- ¹⁵J. T. Groves, L. K. Mahal, and C. R. Bertozzi, *Langmuir* **17**, 5129 (2001).
- ¹⁶B. A. Cornell, V. L. B. Braach-Maksyitis, L. G. King, P. D. J. Osman, B. Raguse, L. Wiczorek, and R. J. Pace, *Nature* **387**, 580 (1997).
- ¹⁷B. Raguse, V. Braach-Maksyitis, B. A. Cornell, L. G. King, P. D. J. Osman, R. J. Pace, and L. Wiczorek, *Langmuir* **14**, 648 (1998).
- ¹⁸L. J. C. Jeuken, S. A. Weiss, P. J. F. Henderson, S. D. Evans, and R. J. Bushby, *Anal. Chem.* **80**, 9084 (2008).
- ¹⁹A. I. Michaloliakos, G.-P. Nikoleli, C. G. Siontorou, and D. P. Nikolelis, *Electroanalysis* **24**, 495 (2012).
- ²⁰M. B. Fritzen-Garcia, V. C. Zoldan, I. R. W. Z. Oliveira, V. Soldi, A. A. Pasa, and T. B. Creczynski-Pasa, *Biotechnol. Bioeng.* **110**, 374 (2013).
- ²¹A. Dahlin, M. Zäch, T. Rindzevicius, M. Käll, D. S. Sutherland, and F. Höök, *J. Am. Chem. Soc.* **127**, 5043 (2005).
- ²²K. Toma, H. Kano, and A. Offenhäusser, *ACS Nano* **8**, 12612 (2014).
- ²³C. A. Keller and B. Kasemo, *Biophys. J.* **75**, 1397 (1998).
- ²⁴E. Reimhult, F. Höök, and B. Kasemo, *Langmuir* **19**, 1681 (2002).
- ²⁵E. Reimhult, M. Zäch, F. Höök, and B. Kasemo, *Langmuir* **22**, 3313 (2006).
- ²⁶A. P. Serro, A. Carapeto, G. Paiva, J. P. S. Farinha, R. Colaço, and B. Saramago, *Surf. Interface Anal.* **44**, 426 (2012).
- ²⁷Z. Peng, J. Tang, X. Han, E. Wang, and S. Dong, *Langmuir* **18**, 4834 (2002).
- ²⁸J. Ekeröth, P. Konradsson, and F. Höök, *Langmuir* **18**, 7923 (2002).
- ²⁹J. Kunze, J. Leitch, A. L. Schwan, R. J. Faragher, R. Naumann, S. Schiller, W. Knoll, J. R. Dutcher, and J. Lipkowski, *Langmuir* **22**, 5509 (2006).
- ³⁰J. T. Marques, R. F. M. de Almeida, and A. S. Viana, *Soft Matter* **8**, 2007 (2012).
- ³¹E. Kalb, S. Frey, and L. K. Tamm, *Biochim. Biophys. Acta* **1103**, 307 (1992).
- ³²P. Nollert, H. Kiefer, and F. Jähnig, *Biophys. J.* **69**, 1447 (1995).
- ³³G. J. Hardy, R. Nayak, and S. Zauscher, *Curr. Opin. Colloid Interface Sci.* **18**, 448 (2013).
- ³⁴S. M. Schiller, R. Naumann, K. Lovejoy, H. Kunz, and W. Knoll, *Angew. Chem. Int. Ed.* **42**, 208 (2003).
- ³⁵X. Wang, M. M. Shindel, S.-W. Wang, and R. Ragan, *Langmuir* **26**, 18239 (2010).
- ³⁶M. Li, M. Chen, E. Sheepwash, C. L. Brosseau, H. Li, B. Pettinger, H. Gruler, and J. Lipkowski, *Langmuir* **24**, 10313 (2008).
- ³⁷N.-J. Cho, S.-J. Cho, K. H. Cheong, J. S. Glenn, and C. W. Frank, *J. Am. Chem. Soc.* **129**, 10050 (2007).
- ³⁸N.-J. Cho, K. K. Kanazawa, J. S. Glenn, and C. W. Frank, *Anal. Chem.* **79**, 7027 (2007).
- ³⁹R. P. Richter, R. Bérat, and A. R. Brisson, *Langmuir* **22**, 3497 (2006).
- ⁴⁰G. Wilemski, *J. Stat. Phys.* **14**, 153 (1976).
- ⁴¹See supplementary material at <http://dx.doi.org/10.1116/1.4945306> for average and standard deviation of QCM-D measurements.
- ⁴²C. Werner, H. Körber, R. Zimmermann, S. Dukhin, and H.-J. Jacobasch, *J. Colloid Interface Sci.* **208**, 329 (1998).
- ⁴³K. Greben, P. Li, D. Mayer, A. Offenhäusser, and R. Wördenweber, *J. Phys. Chem. B* **119**, 5988 (2015).
- ⁴⁴G. J. Brewer, J. R. Torricelli, E. K. Evege, and P. J. Price, *J. Neurosci. Res.* **35**, 567 (1993).
- ⁴⁵A. C. Blakeston *et al.*, *Langmuir* **31**, 3668 (2015).
- ⁴⁶M. Rodahl, F. Höök, A. Krozer, P. Brzezinski, and B. Kasemo, *Rev. Sci. Instrum.* **66**, 3924 (1995).
- ⁴⁷N.-J. Cho, C. W. Frank, B. Kasemo, and F. Hook, *Nat. Protoc.* **5**, 1096 (2010).
- ⁴⁸R. Richter, A. Mukhopadhyay, and A. Brisson, *Biophys. J.* **85**, 3035 (2003).
- ⁴⁹U. Seifert and R. Lipowsky, *Phys. Rev. A* **42**, 4768 (1990).
- ⁵⁰U. Seifert, *Adv. Phys.* **46**, 13 (1997).
- ⁵¹R. F. Tabor, A. J. Morfa, F. Grieser, D. Y. C. Chan, and R. R. Dagastine, *Langmuir* **27**, 6026 (2011).
- ⁵²K. Dimitrievski and B. Kasemo, *Langmuir* **24**, 4077 (2008).
- ⁵³E. Siepi, S. Lutz, S. Meyer, and S. Panzner, *Biophys. J.* **100**, 2412 (2011).
- ⁵⁴J. H. K. Rozenfeld, T. R. Oliveira, M. T. Lamy, and A. M. Carmona-Ribeiro, *Biochim. Biophys. Acta* **1808**, 649 (2011).
- ⁵⁵T. Cha, A. Guo, and X. Y. Zhu, *Biophys. J.* **90**, 1270 (2006).
- ⁵⁶D. Afanasenkau and A. Offenhäusser, *Langmuir* **28**, 13387 (2012).
- ⁵⁷H. Lv, S. Zhang, B. Wang, S. Cui, and J. Yan, *J. Controlled Release* **114**, 100 (2006).
- ⁵⁸P. L. Felgner, T. R. Gadek, M. Holm, R. Roman, H. W. Chan, M. Wenz, J. P. Northrop, G. M. Ringold, and M. Danielsen, *Proc. Natl. Acad. Sci.* **84**, 7413 (1987).
- ⁵⁹A. Csiszár, N. Hersch, S. Dieluweit, R. Biehl, R. Merkel, and B. Hoffmann, *Bioconjugate Chem.* **21**, 537 (2010).
- ⁶⁰R. E. Brown, *Biochim. Biophys. Acta* **1113**, 375 (1992).
- ⁶¹K. Kumar, C. S. Tang, F. F. Rossetti, M. Textor, B. Keller, J. Voros, and E. Reimhult, *Lab Chip* **9**, 718 (2009).
- ⁶²S. Pautot, H. Lee, E. Y. Isacoff, and J. T. Groves, *Nat. Chem. Biol.* **1**, 283 (2005).
- ⁶³Y. K. Lee, H. Lee, and J.-M. Nam, *NPG Asia Mater.* **5**, e48 (2013).
- ⁶⁴N. G. Caculitan, H. Kai, E. Y. Liu, N. Fay, Y. Yu, T. Lohmüller, G. P. O'Donoghue, and J. T. Groves, *Nano Lett.* **14**, 2293 (2014).